Edge Plasma Experiments on CASTOR Tokamak *

Žáček F., Stöckel J., Badalec J., Jakubka K., Kletečka P., Kryška L., Kříha V. †, Svoboda V. ‡, Petržílka J. §, Voitsekhovich I. ¶, Dhyani V. ‖

Institute of Plasma Physics
Czech Academy of Sciences
Za Slovankou 3, P.O.Box 17, 182 11 Prague 8
Czech Republic

Abstract

We present a short survey of main experimental activities on the small tokamak CASTOR (IPP Prague). This activity concerns investigation of edge plasma fluctuations to specify better the processes resulting in an improvement of the global particle confinement, observed in CASTOR with lower hybrid current drive and plasma edge polarization.

IPPCZ - 332

March 1993

*This report was presented on KFA-IPP-KFKI-RMKI Joint Workshop on "Use of Atomic Beams in Plasma Experiments", Budapest, 29 March - 2 April 1993

†Faculty of Electrotechnics, Czech Technical University, Prague

‡Faculty of Nuclear Engineering, Czech Technical University, Prague

§Mat. Phys. Faculty, Charles University, Prague

¶Kurchatov Institute, Moscow, Russia

‖Cultural Exchange Programme between Czech Republic and India

1 Introduction

The important role of the edge plasma in the global particle and energy balance in tokamaks is well recognized. However, the complexity of all processes involved in the particle and energy losses hinders to create an appropriate theoretical model of anomalous transport in tokamaks up to now. It seems to be evident only that the anomalous transport relies in the turbulent character of tokamak periphery. However, complete and exhaustive experimental data from the tokamaks periphery are still necessary.

The main aim of the experimental research on tokamak CASTOR is focussed to investigations of the edge plasma characteristics in the regimes with the improved confinement. Such regimes are reached in CASTOR with lower hybrid current drive or by plasma edge polarization [1,2]. Results of these investigations indicate that the link between the global confinement and the level of edge fluctuations is more complex than it is generally assumed. The contribution brings a short survey of experimental activities undertaken on the tokamak CASTOR in this direction.

2 Experiments

Tokamak CASTOR is a small device with $R/a = 0.4m/0.1m$, toroidal magnetic field $B_T \leq 1.5T$, plasma current $I_P \leq 30kA$, $\bar{n}_e \leq 2 \cdot 10^{19} m^{-3}$ and pulse duration $\tau \leq 40ms$. The vacuum chamber has six diagnostic crosses, all with two vertical and one horizontal ports. For the experiment with lower hybrid current drive (LHCD) the magnetron generator with the power $P_{LH} \leq 50kW$ and frequency $f = 1.25GHz$ is used. A multijunction grill with mouth dimensions $160 \times 50mm$ serves as a launching antenna. For the edge plasma polarization an insulated limiter or a massive graphite electrode, immersed into the edge plasma, were biased using a thyristor modulator ($U \leq 300V$, $I \leq 100A$).

The following diagnostics are employed for the measurements of the global particle confinement and fluctuations of the edge plasma:

1. 4-channel interferometr ($\lambda = 4mm$) for measurement of the line-average electron density.

2. Registration of the H_α and impurity spectral lines intensities in several parts of vacuum chamber to estimate an influx of particles for determination of the particle confinement time [3].

3. Langmuir probes for determination of the edge plasma parameters:

   - single, double and triple Langmuir probes for measurements of radial profiles on the shot to shot basis; they are distributed poloidally and toroidally around the torus;
   - a set of poloidally distributed triple probes fixed in one cross-section for measurement of poloidal asymmetries in the fluctuation-induced radial particle fluxes [4];

- a rake of 16 probes for mapping of the edge plasma;
- a fast rotating probe for measurement of radial profiles during a single shot [5];
- an oscillatory probe for the measurement of electron temperature unaffected by existence of poloidal electric fields.

The probe data have been processed either by an analog correlation technique or by digitizing.

4. A set of 16 poloidally distributed Mirnov coils for measurement of poloidal magnetic field fluctuations [6].

5. Low energy Li beam diagnostics for measurement of density profiles [7].

3 Brief survey of activities and main results

3.1 Fluctuation-induced radial particle fluxes during LHCD

It was found from Langmuir probes data that the fluctuation-induced flux $\tilde{\Gamma}$ of particles has outward direction and it is quite comparable with the flux determined from the global particle balance in tokamak CASTOR [4]. This flux $\tilde{\Gamma}$ drops substantially during LHCD period of a discharge due to the reduction of both density $\tilde{n}_e$ and poloidal electric field fluctuations $\tilde{E}_p$ levels as well as due to decrease of their mutual correlation. The situation is illustrated in Fig. 1, where the time evolutions of all this quantities together with the line average electron density $\bar{n}_e$ are plotted. Simultaneously a significant increase of the global particle confinement is observed [3].

The mechanism responsible for the reduction and decorrelation of electrostatic fluctuations during LHCD is quite not straight-lined (an attempt to find it is made in the next paragraph).

3.2 Possible role of runaway electrons in the improvement of particle confinement during LHCD

The reduction of fluctuations and the corresponding improvement of global particle confinement during LHCD is not proportional to the LH driven current I_{LH}. It is demonstrated in Fig. 2, which presents the LH power dependence of the relative reduction of edge density fluctuations $\Delta = (\tilde{n}_e^{OH} - \tilde{n}_e^{LH})/\tilde{n}_e^{OH}$, the normalized particle confinement τ_{LH}/τ_{OH} and the LH wave driven current I_{LH} for a total plasma current $I_P = 12kA$. It is possible to see that the effect has no power threshold and that the best confinement and a maximum reduction of fluctuations is reached already at moderate LH power, when $I_{LH} \simeq I_P/2$ and therefore the residual loop voltage is still far above zero (about one half of its initial OH value). On the basis of this fact the following model explaining the behaviour of the measured reduction of fluctuations in the LH power scan is proposed:

1. The runaway electrons are populated during LHCD with enhanced rate if their threshold energy $W_{run} \sim n/U_{loop}$ occurs within the interval of LH wave energy spectrum (W_1, W_2), i.e. if $W_1 < W_{run} < W_2$.

2. Non-ambipolar losses of the runaway electrons lead to positive charging of the plasma; the intensity of the arising radial electric field is proportional to the number of runaway electron population.

3. Due to this edge radial electric field the plasma poloidal rotation increases and consequently the edge fluctuations (and the particle transport) are reduced.

4. The number of populated runaway electrons increases with LH power until U_{loop} is so low that $W_{run} \simeq W_2$. Afterthat the rate of runaway electron population decreases. It results in observed decrease of fluctuations reduction if LH power is further increasing.

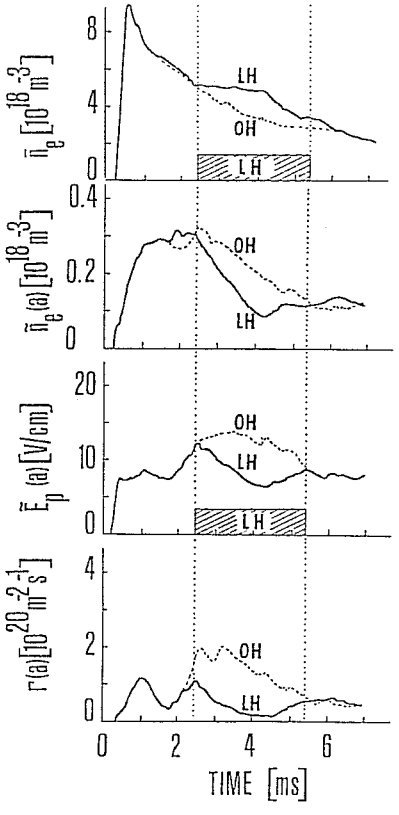

Fig. 1

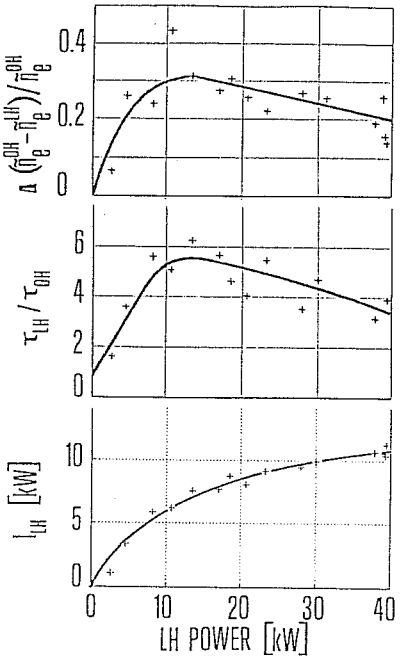

Fig. 2

Figure 1: Comparison of fluctuating peripheral parameters $\tilde{n}_e$, $\tilde{E}_p$ and $\tilde{\Gamma}$ on the limiter radius a, together with line average density $\bar{n}_e$ in OH and LHCD regimes.

Figure 2: The power dependence of relative reduction of edge density fluctuations, increase of normalized particle confinement and value of LH driven current.

3.3 Profiles of radial electric field and poloidal velocity of plasma fluctuations during LHCD

The poloidal rotation of the plasma seems to play an important role in the fluctuation-induced radial particle flux in tokamaks. Especially the shear of rotation velocity, existing in the vicinity of the last closed flux surface ($LCFS$), could exhibit a strong decorrelation effect on fluctuations. An existence of such velocity shear layer in tokamak CASTOR is illustrated in Fig. 3. The figure depicts a cross correlation function of two fluctuating signals registered by two insulated Langmuir probes, separated poloidally by a distance 5 mm, and shifted together radially in stepwise fashion between OH shots. Time delay (in μs) is on the horizontal axis, r is the radial position of probes. The velocity v_p of potential fluctuations can be derived from the delay of the maximum of the cross correlation function and probe separation. It is possible to see, that shear layer is located slightly inwards of the limiter radius a. On the outer side of the layer (in the limiter shadow) the fluctuations are rotating in the direction of ion diamagnetic drift, deeper inside the plasma the direction of the rotation is opposite.

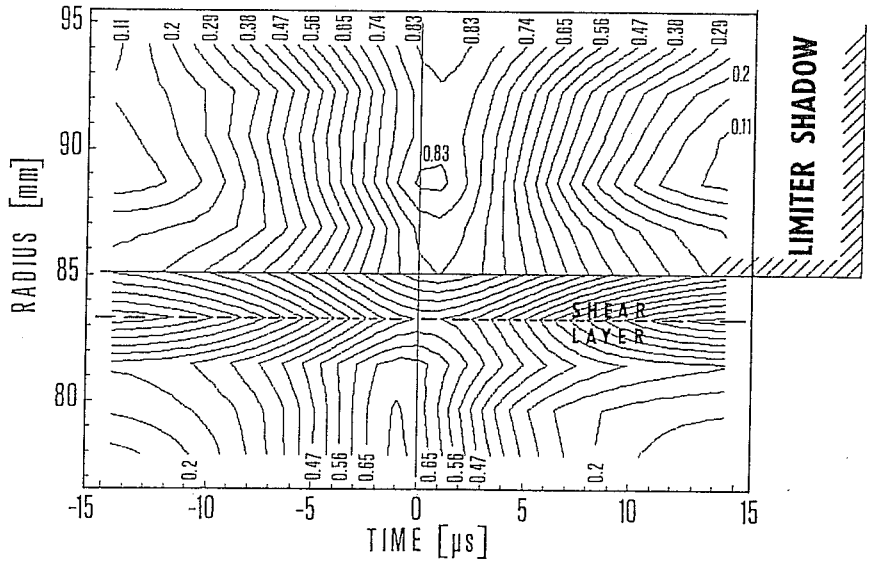

Figure 3: A radial map of cross-correlation function of plasma floating potential registered by two Langmuir probes with poloidal separation 5mm.

In the case of LHCD, the velocity of poloidal rotation generally increases and the shear layer starts to move outwards, see Fig. 4 [8]. In this figure the temporal evolutions of v_p for three different probe radial positions are compared with the OH case. The motion of the shear layer through the radius $r = 84mm$ during LHCD is evident.

The poloidal rotation of fluctuations is a consequence of an existence of the radial electric field ($\vec{E}_r \times \vec{B}_T$). The form of the edge radial electric field (measured by the rotating probe) can be deduced from Fig. 5., where the radial profile of plasma floating potential V_F just before and during LHCD are compared. The shift of the

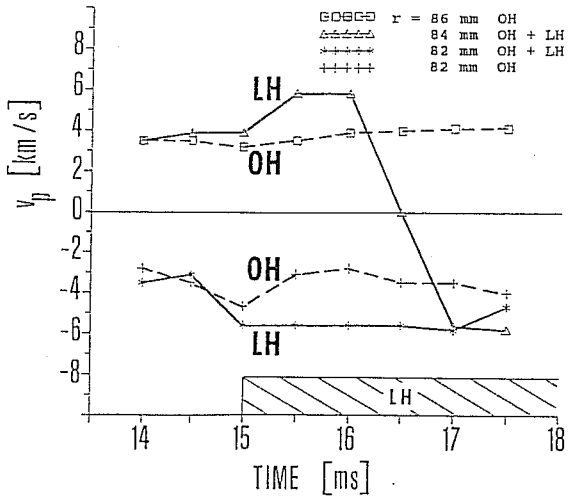

Figure 4: Time evolution of poloidal velocity v_p at three different probes radius in OH and LHCD regimes (poloidal separation of the probes 7mm).

layer with $E_r = 0$ and increase of the radial electric field in scrape-off layer (SOL) with LHCD are apparent.

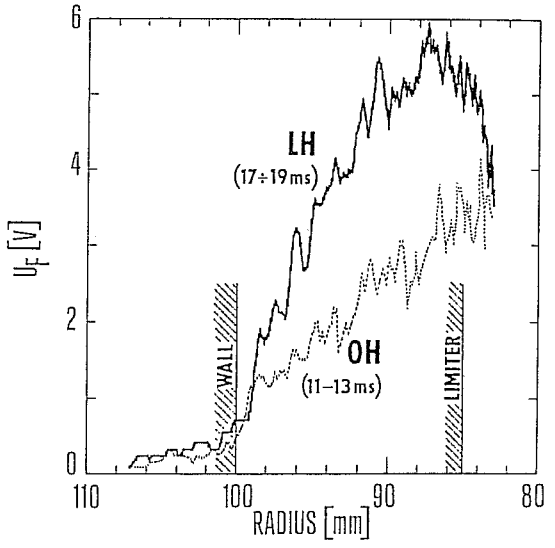

Figure 5: Comparison of radial profiles of the plasma floating potential in OH and LHCD regimes.

3.4 Dimensional analysis of density fluctuations in OH and LHCD regimes

The question whether the plasma fluctuations are stochastic (i.e. if they have a turbulent character with an infinite degrees of freedom) or if they are deterministic in some degree can be solved by the dimensional analysis. This technique consists in

computing of the correlation dimension D, which is a measure of the deterministic chaos in dynamic systems [9]. The results of such computation for probe fluctuating data in OH and LHCD regimes are shown in Fig. 6 (for details see [10]). Here N denotes number of experimental data (sampling frequency 5 MHz), d is the chosen time delay, M is the number of reference points and n is the embedding dimension. To check the correctness of the method, results of calculation for random data (white noise) are plotted in the same figure as well. Because $D < n$, we conclude, that the value D calculated for the measured fluctuations have to be taken only as the lowest estimate of the correlation dimension. Nevertheless, it may be seen that the correlation dimension in the LHCD regime is always higher then in the ohmic phase. This suggests that the fluctuations are more stochastic in this case (closer to the white noise). It was found, however, that the computed value of the correlation dimension is inversely proportional to the autocorrelation time for our data. Therefore, the reliability of the Grassberger-Procaccia algorithm [9] to compute the correlation dimension for our limited set of data is now under revision.

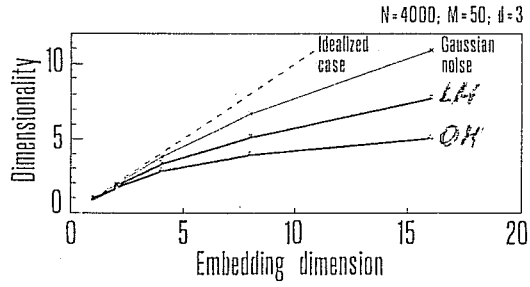

Figure 6: Comparison of calculated correlation dimensionality D for OH and LHCD regimes in dependence on the chosen embedding dimension n.

3.5 Radial profiles of electron density in LHCD regime

The knowledge of electron density profile in real tokamak experiments is a fundamental requirement to calculate the transport coefficients. The Fig. 7 shows a comparison of the density profiles $n_e(r)$ in OH and LHCD regimes measured on the CASTOR tokamak using a low energy Li beam diagnostics [7]. It may be seen that

- radial distribution of the electron density in the OH regime of tokamak CASTOR can be described quite well by a simple parabolic profile;
- a region with a steep density gradient is formed approximately in the half of tokamak chamber radius during LHCD; this region represents an additional transport barrier separating the hot plasma core from the periphery;
- despite of an increase of total number of particles in the tokamak, the local density in peripheral regions is slightly lowerized during the LHCD; a certain broadening of the density profile in the central part of the plasma during the LHCD, characterized by a parabola of higher order, can be deduced from this fact.

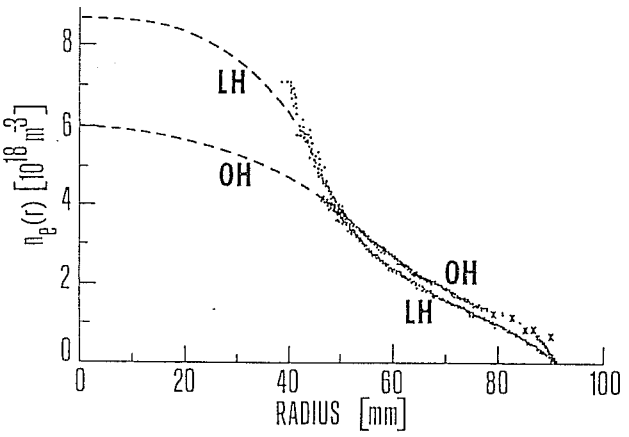

Figure 7: Radial profiles of electron density in OH and LHCD regimes of tokamak CASTOR operation.

3.6 Comparison of regimes with LHCD and edge plasma polarization

Using a biased electrode or limiter, the radial current flowing across the outer magnetic surface can be generated. In this way a modification of the edge radial electric field can be induced with consequences on the level and character of plasma fluctuations [11].

Fig. 8 comparises the radial profiles of quantities characterizing the density fluctuations $\tilde{n}$ in LH and EP with the OH regimes. For the edge polarization the positively biased electrode located at radius $r_E/a = 0.8$ was used. Due to its relative small surface the electrode current was below $10A$ and the global particle confinement has remained on the ohmic level. Nevertheless, it may be seen from the figure that the density fluctuations are noticeably reduced in both cases up to 50% of the standard ohmic value inside the whole SOL. The relative level of $\tilde{n}/n$ decreases significantly during the EP while it remains close to the initial value in LHCD regime. Simultaneously a significant increase of the poloidal velocity v_p near LCFS and decrease of fluctuations autocorrelation time τ_c^{LAB} are observed throughout the SOL, which is consistent with the floating potential measurements indicating an increase of radial electric field inside SOL in both regimes (see Fig. 5 e.g.).

To generate higher radial currents, the limiter has been also used as a biasing electrode. It was found that after reaching $60A$ the limiter current suddenly drops and a transition to the improved particle confinement occurs. Measurement of turbulent characteristics of discharges with limiter biasing are in progress.

3.7 Some general features of the periphery turbulent characteristics

Some common characteristics of the periphery can be drawn using the correlation technique. In Fig. 9 the relative levels of density fluctuations $\tilde{n}/n$ versus velocity of their poloidal rotation v_p are displayed. The data are taken from a set of CASTOR

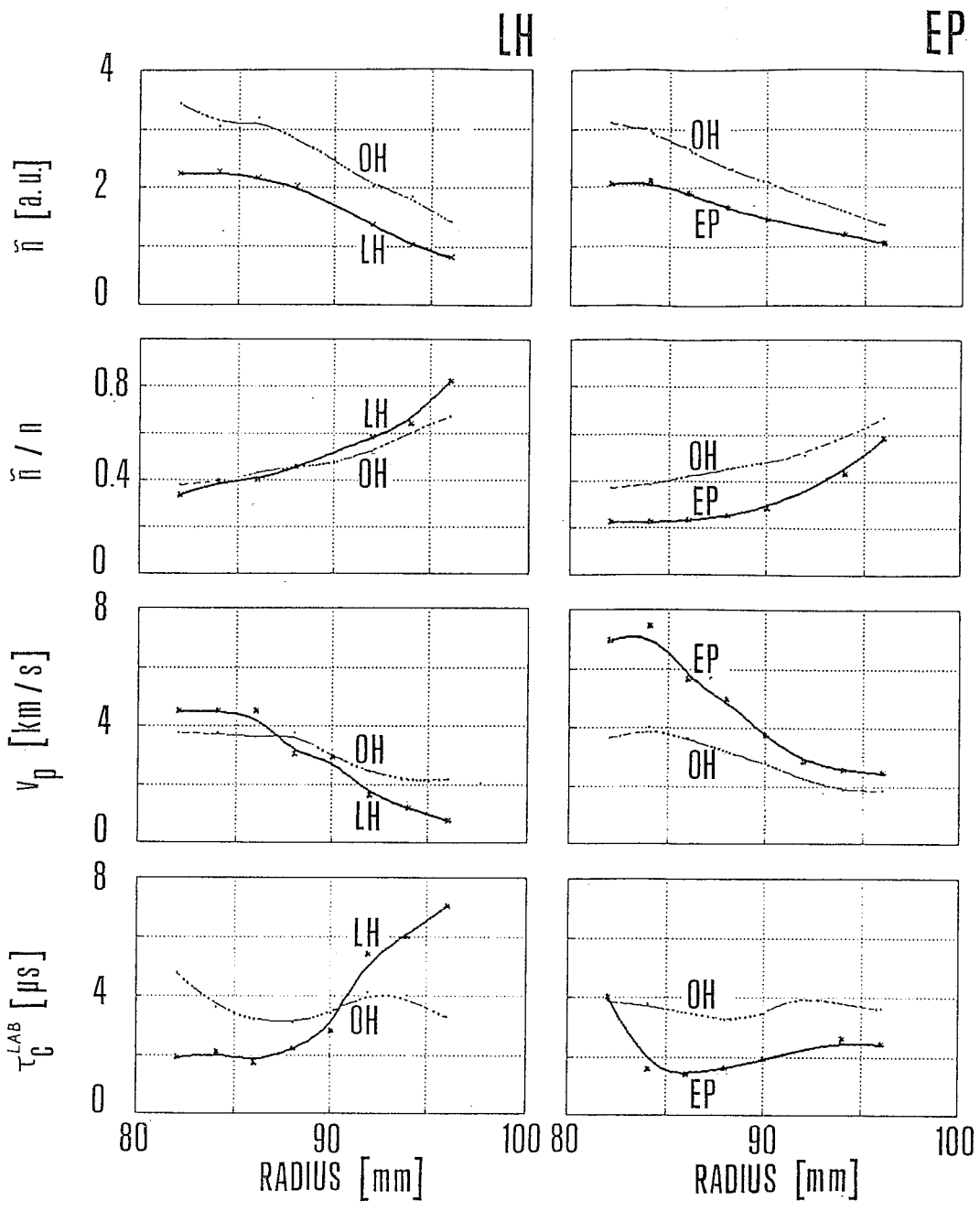

Figure 8: Comparison of radial profiles of fluctuation levels (both absolute and relative), propagation velocity in poloidal direction and the width of the autocorrelation function in OH, LHCD ($P_{LH} = 20kW$) and EP ($U_b = +200V$) regimes.

discharges, regardless on the probe position and type of measured dependence (see figure caption). A well expressed correlation between these two quantities in the form of exponential dependence $\tilde{n}/n \simeq exp(-v_p/v_o)$ with $v_o \simeq 5km/s$ can be seen.

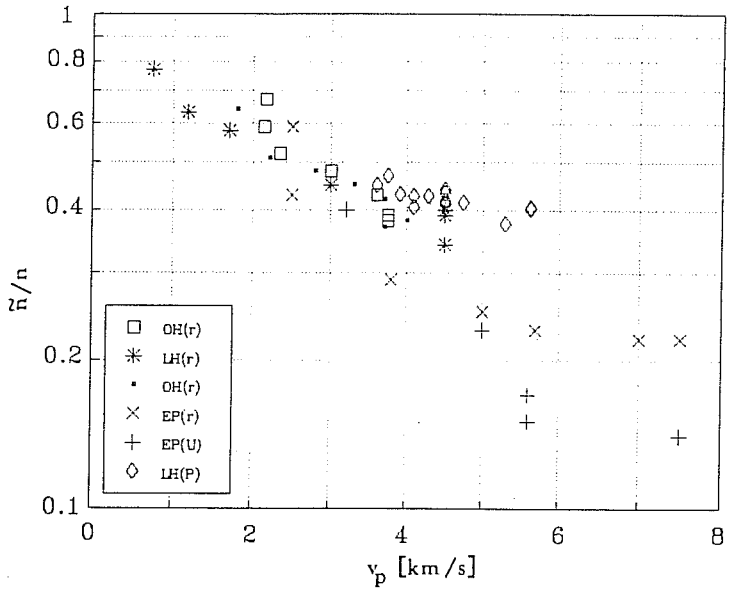

Figure 9: Relation between the relative level of density fluctuations in SOL and their poloidal velocity obtained during measurements of the following dependences:
$OH(r)$ ... radial dependences in OH regimes
$LH(r)$ ... radial dependences in LHCD regimes
$EP(r)$ ... radial dependences in experiments with plasma edge polarization
$EP(U)$ ... dependence on the voltage used for the plasma edge polarization
$LH(P)$ ... dependence on the LH power.

An other relevant result about the time-space properties of the edge fluctuations has been deduced by the transition from the laboratory to the rest frame. Under assumption of a Gaussian form of fluctuating structures both in time and space, a simple relation between the autocorrelation time in the laboratory τ_c^{LAB} and rest τ_c^{REST} frames can be derived [12]:

$$(1/\tau_c^{LAB})^2 = (1/\tau_c^{REST})^2 + (v_p/\lambda_c)^2,$$

where λ_c is the correlation length and v_P the measured poloidal velocity of fluctuations. To estimate the autocorrelation time, unaffected by the rotation, the data at several probe positions (from Fig. 8) are plotted in Fig. 10 in the form $(1/\tau_c^{LAB})^2$ versus v_p^2. It is possible to see that dependences are three lines with different (but constant) slope $(1/\lambda_c)^2$, from which the correlation length can be estimated. The quotient $(1/\tau_c^{REST})^2$ represents the real correlation time of density fluctuations. The linear form of dependencies suggests that the correlation length and time of the fluctuations are constant throughout the SOL. The electrostatic fluctuations can be therefore describes in SOL in every regime as fast changing, but compact formations.

It may be seen from the Fig. 10 that the correlation characteristics of described fluctuating formation are substantially modified by both LHCD and EP applications,

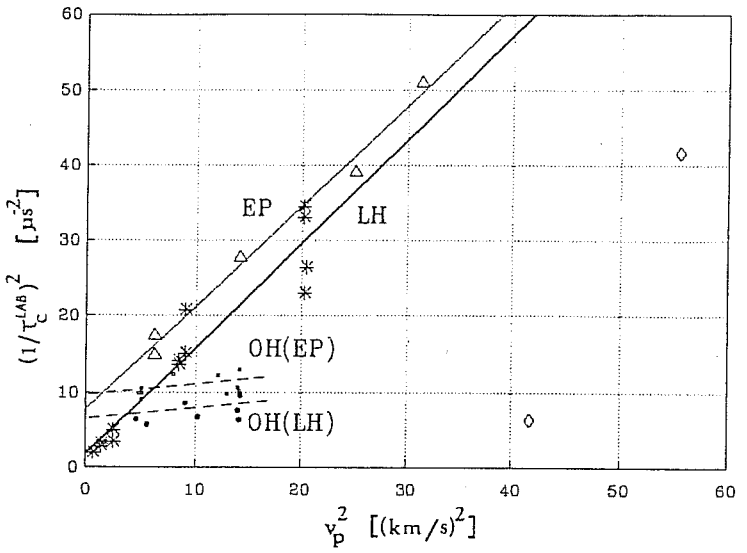

Figure 10: Plot of autocorrelation time in the laboratory frame versus propagation velocity of density fluctuations.

independently on the fact, if the improvement of global particle confinement is observed or not. However, this modification has a different character: while the correlation length decreases substantially in both cases (from about 30 to 10mm), the correlation time changes in the case of LHCD only (increases from about 4 to 8 μs).

Acknowledgements

The work was performed under Grants of Czechoslovak Academy of Sciences No 14308 and 14310 and was supported also by the IAEA Contract No 6702/RB.

References

[1] Stöckel J. et al.: "Edge fluctuations at regimes with improved confinement on CASTOR tokamak", 19th EPS Conf. on Contr. Fusion and Plasma Physics, Innsbruck 1992, Proc. I, p. 219

[2] Žáček F. et al.: "Edge plasma turbulent characteristics on the CASTOR tokamak", 14th Internat. Conf. on Plasma Phys. and Controlled Nucl. Fus. Res., IAEA-CN-56/A-3-8, Oct 1992, Würzburg

[3] Badalec J. et al.: "Regimes with improved particle confinement on CASTOR tokamak", IAEA TCM on Research Using Small Tokamaks, Sept. 1992, Würzburg

[4] Stoeckel J. et al.: "Studies of electrostatic and magnetic fluctuations in CASTOR tokamak", 13th Internat. Conf. on Plasma Phys. and Contr. Nucl. Fus. Research, Washington 1990, Nucl. Fus. Supplement 1991, Vol. I, 491

[5] Stoeckel J. et al.: "Rotating Langmuir probe for measurement of edge radial profiles on CASTOR tokamak", IAEA TCM on Research Using Small Tokamaks, Oct 1991, Hefei, China, Proc. 204-211

[6] Valovič M.: "Suppression of magnetic fluctuations by lower hybrid current drive on the CASTOR tokamak", IPPCZ-300, Prague, May 1990

[7] Jakubka K. et al.: "Diagnostic Arc Source of Neutral Lithium Beam", IAEA TCM on Research Using Small Tokamaks, Sept. 1992, Würzburg

[8] Žáček F. et al.: "Density fluctuations and particle confinement during OH/LHCD on tokamak CASTOR", 18th EPS Conf. on Contr. Fus. and Plasma Physics, Berlin 1991, Proc. Vol. III, 341

[9] Grassberger P. et al.: Phys. Rev. Let. 50 (1983), 346

[10] Stöckel J. et al.: "Correlation and dimensional analysis of density fluctuations on CASTOR tokamak", IAEA TCM on Research Using Small Tokamaks, Sept. 1992, Würzburg

[11] Taylor R.J. et al.: "H-mode behavior induced by cross-field currents in a tokamaks", Phys. Rev. Let. 63 (1989), 2365

[12] Vayakis G., Rep. AEA FUS 123, Culham 1991